

Towards the introduction of magnetic resonance guided stereotactic body radiotherapy for the treatment of prostate cancer

A thesis submitted in the fulfilment
of the requirements of the degree of Master of Science

in

Technical Medicine
Medical Imaging and Intervention

Author:
Iris HAMELINK

Graduation Committee:
Prof. dr. ir. C.H. SLUMP
Dr. ir. A.W.H. MINKEN
Dr. K. MULLER
Dr. M. GROENIER

October 21, 2020

**UNIVERSITY
OF TWENTE.**



Abstract

Introduction

The main challenge in radiotherapy (RT) is ensuring that the dose to the surrounding tissue is kept as low as possible while delivering a relatively high dose to the tumor. Currently, the clinical introduction of magnetic resonance imaging (MRI) guided RT might enable more effective tumor targeting while sparing the surrounding tissue as much as possible. Especially treatment of prostate carcinoma might benefit from this, since accurate dose delivery is highly influenced by interfractional motion and deformation of the prostate gland. Before introducing MR guided prostate RT within the clinical practice, it should be clear whether it actually leads to improved sparing of organs at risk (OAR) and target coverage compared to cone beam computed tomography (CBCT) guided prostate RT.

Objective

The aim of this study is to quantify the (theoretical) clinical added value of the use of MR accelerator (e.g. MR-Linac) systems by comparing planning options for MRI guided RT versus CBCT guided RT for the treatment of prostate carcinoma.

Keywords: adaptive radiotherapy, MR-Linac, planning study, prostate carcinoma

Preface

Last year, I had the opportunity to conduct research at the Radiotherapiegroep in Deventer and Arnhem (the Netherlands). This included a graduation internship for the degree of Master of Science in Technical Medicine: Medical Imaging and Intervention. This thesis is the written result of the work that has been done in the past year. The aim was to investigate whether the implementation of the MR-Linac can be beneficial for patient with low- to intermediate risk prostate carcinoma.

Two planning simulation studies were conducted. During the past year, I could count on a lot of guidance. I want to express my gratitude towards drs. M.A.D. Haverkort for her clinical guidance and feedback during our numerous meetings. Appreciation extends also towards dr.ir. D. Schuring who was involved in my graduation project. I would like to thank dr. L.G.W. Kerkmeijer en dr.ir. E.J.L. Brunenberg for their input and feedback during our meetings and for allowing me to use their Radboudumc resources.

I want to give special thanks to my supervisors, who helped me realizing this graduation internship. My supervisors at the Radiotherapiegroep: dr. K. Muller and dr.ir. A.W.H. Minken. Thank you for your clinical guidance, support during the COVID-19 crisis and feedback sessions. And last but not least, my supervisors at the University of Twente. Prof.dr.ir. C.H. Slump and dr. M. Groenier, thank you for our conversations and feedback discussions.

Finally, I want to thank my family and friends for showing interest and support during the past year.

Iris Hamelink
October 21st, 2020

Contents

1	Introduction	1
2	Feasibility of stereotactic body radiotherapy for prostate carcinoma on a 1.5T magnetic resonance imaging guided linear accelerator	3
2.1	Introduction	3
2.2	Materials and methods	3
2.2.1	Patients	3
2.2.2	Radiotherapy simulation and contouring	3
2.2.3	Treatment planning strategy	4
2.2.4	Intensity Modulated Radiotherapy	4
2.2.5	Volumetric Arc Therapy	4
2.2.6	Data analysis	4
2.3	Results	5
2.4	Discussion	5
2.5	Conclusion	7
3	Towards online adaptive replanning with the Elekta Unity MR-Linac for extremely hypofractionated prostate carcinoma radiotherapy treatment	8
3.1	Introduction	8
3.2	Methods and materials	8
3.2.1	Patients	8
3.2.2	Radiotherapy simulation and contouring	9
3.2.3	Pre-treatment planning strategy	9
3.2.4	Fiducial marker based position verification	10
3.2.5	Adaptive treatment planning strategy	10
3.2.6	Dosimetric evaluation	10
3.3	Results	10
3.4	Discussion	12
3.5	Conclusion	13
4	Conclusion	14
5	Future perspectives	15

List of Figures

1	The dose distributions of a) fiducial marker (FM) position verification, b) adaptive replanning using a 5 mm CTV to PTV margin.	5
2	The dose distributions of a) fiducial marker (FM) position verification and b) adaptive replanning (AR) using a 5 mm CTV to PTV margin.	11
3	The dose distributions of a) fiducial marker (FM) position verification, b) adaptive replanning (AR) using a 5 mm CTV to PTV margin and c) AR using a 3 mm CTV to PTV margin.	11

List of Tables

1	EAU risk groups for biochemical recurrence of localized and locally advanced prostate cancer [1].	1
2	Clinical target and OAR constraints	4
3	Dosimetric results of conventional linac VMAT and MR-Linac IMRT treatment plans	6
4	Clinical target and OAR constraints	9
5	Dosimetric results of fiducial marker (FM) position verification and adaptive replanning (AR)	11

List of Abbreviations

AR	adaptive replanning
ATP	adapt to position
ATS	adapt to shape
BT	brachytherapy
CBCT	cone beam computed tomography
CTV	clinical target volume
CT	computed tomography
DVH	dose-volume histogram
EBRT	external beam radiation therapy
ED	electron density
EPID	electronic portal imaging device
ERE	electron return effect
FM	fiducial marker
GTV	gross target volume
Gy	Gray
HDR-BT	high dose rate brachytherapy
hypo-FLAME	hypofractionated focal Lesion ablative microboost in prostate cancer
IGRT	image guided radiotherapy
IMRT	intensity modulated radiotherapy
ISUP	International Society of Urological Pathology
Linac	linear accelerator
MR-Linac	magnetic resonance linear accelerator
MRCAT	magnetic resonance for calculation attenuation
MRI	magnetic resonance imaging
MR	magnetic resonance
OAR	organ at risk
PCa	prostate carcinoma
PSA	prostate-specific antigen
PTV	planning target volume
R-IDEAL	radiotherapy - idea, development, exploration, assessment, and long-term evaluation
RT	radiotherapy
VMAT	volumetric arc therapy

1 Introduction

In the Netherlands, PCa is the most commonly diagnosed cancer in men and represents 22% of all new malignancies in men [2]. More than half of all patients is >70 years and approximately 60% of diagnosed prostate cancers are not metastasized [3]. Based on tumor risk factors, PCa can be classified into three risk groups, as depicted in Table 1. The classification is based on the guidelines of the European Association of Urology (EAU) [1].

Table 1: EAU risk groups for biochemical recurrence of localized and locally advanced prostate cancer [1].

Definition			
Low risk	Intermediate risk	High risk	
PSA <10 ng/mL	PSA 10-20 ng/mL	PSA >20 ng/mL	any PSA
GS <7 (ISUP grade 1)	or GS 7 (ISUP grade 2/3)	or GS >7 (ISUP grade 4/5)	any GS (any ISUP grade)
and cT1-2a	or cT2b	or cT2c	cT3-4 or cN+
Localized			Locally advanced

GS = Gleason score; ISUP = International Society of Urological Pathology; PSA = prostate-specific antigen.

Current standard treatment options for patients with localized low and intermediate risk PCa include active surveillance (mainly for low risk PCa), radical prostatectomy, external beam radiation therapy (EBRT) or brachytherapy. Since the survival rate is comparable for all options, the choice of treatment is based upon the probability of developing long-term side effects and the preference of the patient [4].

Modern EBRT techniques include fiducial marker (FM) implantation, MR based delineation, Intensity Modulated RT (IMRT) or Volumetric Arc Therapy (VMAT) and daily electronic portal imaging device (EPID)/cone beam computed tomography (CBCT) position verification. The FMs are implanted in the prostate gland prior to RT. These markers are considered as a surrogate for the target area [5]. Subsequently, a planning computed tomography (CT) scan and a magnetic resonance imaging (MRI) scan are acquired. The CT scan provides electron-density information for treatment planning, while the MRI scan provides improved soft-tissue contrast [5]. For imaging and contouring of the prostate for radiotherapy planning purposes, MRI has shown to be superior to CT [6]. Therefore, the prostate is delineated on the MRI, which is rigidly registered based upon FM position with the CT scan. The subsequent treatment plan is made on the CT. To ensure accurate irradiation of the tumor and prostate and sparing of organs at risk (OAR), target position verification in EBRT is based upon the position of the gold FMs. By using the FM position on daily CBCT or EPID as a surrogate for the prostate, set-up errors and internal motion of the prostate relative to the bony anatomy can be identified [7].

Recent literature shows that extreme hypofractionation (5 fractions) of dose delivery in low and intermediate risk PCa patients yields excellent disease-free survival and low rates of severe toxicity [8][9][10][11][12]. Since the tumor is surrounded by OAR, particularly the rectal wall and bladder, the targeting of an extremely hypofractionated radiation dose should be precise. Precision of FM based position verification is high, with the possibility to position within systematic and random position errors of <1 mm [13]. However, the effectiveness of this method relies on the fixation of the FMs within the prostate, the absence of significant deformation and rotation of the prostate during the course of treatment and the accuracy of marker position verification [7]. Deformation of the prostate arises as a consequence of RT treatment. Deformation can occur due to temporary prostate edema or to the mass effect from surrounding structures. Additionally, rectal filling appears to induce rotation and deformation of the prostate. [14]

In the past few years, integrated MRI accelerator systems (e.g. MR-Linac) have been developed, enabling use of the soft-tissue contrast of MRI to image the patient before and during radiotherapy delivery [15]. The available MRI accelerator systems combine a hybrid MRI and radiotherapy system (i.e. a linear accelerator) [16][17]. These systems have the potential to provide real-time soft-tissue

imaging during radiation delivery and as such allow tumor tracking for better targeting precision [18]. Due to the improved soft-tissue contrast compared to CBCT based RT, MRI based RT enables the ability to perform daily adaptive replanning on the anatomy of the day [15]. Deformation and rotation of the prostate gland result in large margins around the RT target area to ensure target coverage. Therefore, daily adaptive replanning with MR based RT could ensure more effective tumor targeting while sparing the surrounding tissue as much as possible [19]. The MRI accelerator systems have the potential to offer real-time high precision radiotherapy as a non-invasive treatment of the prostate without the use of fiducial prostate markers [20].

The ability to use online adaptive MRI based RT will possibly enable diminution of radiotherapy margins, reducing toxicity and enabling future dose escalation to increase tumor control rates. However, introduction of the MR-Linac for treatment of PCa in the clinical setting requires a scientifically based approach [21]. This thesis aims to investigate strategies to achieve accurate MRI based RT to facilitate future clinical implementation of the MR-Linac within the Radiotherapiegroep and Radboudumc. It focuses on dosimetric accuracy obtained during planning studies for the MR-Linac. Treatment planning for the MR-Linac differs from the state-of-the-art treatment planning for the conventional linac [22]. Technical differences of the MR-Linac might lead to a deterioration in quality of the dose distribution in treatment planning. Additionally, the clinical feasibility to ensure target coverage and OAR sparing during online adaptive replanning for PCa with MR-Linac is still uncertain. A treatment planning study was carried out to quantify this potential benefit and to further investigate online adaptive treatment planning methods.

2 Feasibility of stereotactic body radiotherapy for prostate carcinoma on a 1.5T magnetic resonance imaging guided linear accelerator

2.1 Introduction

In recent years, several systems integrating a linear accelerator with MRI became commercially available. One of the available systems for the clinical practice is the 1.5 Tesla (T) Unity MR-Linac system (Elekta AB, Stockholm, Sweden) [23]. Due to the integration of the linear accelerator (linac) with MRI, the MR-Linac has technical differences compared to conventional linacs. The presence of the 1.5T magnetic field will cause a phenomenon called the electron return effect (ERE), in which secondary electrons curl and potentially affect the dose distribution. The ERE is mostly observed at the boundaries of tissues with large differences in density and might influence local dose. This effect may potentially also influence rectal dose, due to the presence of air pockets. [24] Additionally, the couch integrated in the Unity MR-Linac system contains dense rails resulting in large dose attenuation. Therefore, the gantry angles $100^\circ - 140^\circ$ and $220^\circ - 260^\circ$ need to be avoided as well as the $8^\circ - 18^\circ$ gantry angles due to the presence of the cryostat-pipe. Additional differences compared to a conventional linac include a nominal flattening filter free beam energy of 7 MV, a fixed collimator angle, collimator leaves that travel in CC direction, a 7 mm leaf width at isocenter and only IMRT delivery. [23]

Based on the R-IDEAL framework [21] for a systematic clinical evaluation of technical innovation in radiation oncology, this study is classified as a stage 0 study. This stage covers all research before the innovation is ready for clinical introduction, including studies concerning the expected benefit of the new technique. The purpose of this study was to investigate whether similar dose distributions for extreme hypofractionated treatment of PCa can be achieved for MR-Linac IMRT planning compared to conventional linac VMAT planning, taking the treatment planning limitations and presence of the 1.5T magnetic field of the Unity MR-Linac into account.

2.2 Materials and methods

2.2.1 Patients

Data of five randomly selected patients treated within the hypo-FLAME study at the University Medical Centre Utrecht was available for this retrospective treatment planning study. For each

included patient, a planning CT and MRI were available. The hypo-FLAME study was approved by the institutional review board and informed consent included approval to use the acquired data for future studies. [25]

2.2.2 Radiotherapy simulation and contouring

Prior to radiotherapy treatment, four FMs were implanted in the prostate by the radiation oncologist using ultrasound guidance. A planning CT and MRI scan were performed in supine position. Patients were advised to have a comfortably full bladder prior to planning CT and MRI acquisition. The planning CT was rigidly registered with the MRI based on the FMs for delineation of the prostate and OAR.

The volumes of interest were defined in agreement with ICRU 62 [26]. To minimize possible errors for both the delineation of the prostate and the relevant normal tissues from interobserver variation, all target volumes were delineated by one observer and this delineation was supervised by a radiation oncologist. The prostate gland as visible on MRI was contoured as gross tumor volume prostate (GTV_P) and the clinical target volume prostate (CTV_P) was defined as $GTV_P + 0$ mm margin. In all five cases seminal vesicle (SV) invasion was present, necessitating delineation of the GTV_{SV} . The GTV_{SV} included the base of the SV plus any region at risk of microscopic extension. The base of the SV was defined as the 2 cm of the SV from the base of the prostate in the axial view. The GTV_P and GTV_{SV} were delineated based on clinical findings and the planning MRI by the observer supervised by a radiation oncologist. To account for systematic positioning errors and intrafraction prostate gland motion due to changes in rectal filling, both PTV_P and PTV_{SV} include a $CTV + 5$ mm isotropic margin.

Delineation of the organs at risk included the rectum, anal canal, bladder, penile bulb, sigmoid, femoral heads and the small bowel. The anorectal contour was defined by the external sphincter to the rectosigmoid flexure or the level of the inferior border of the sacroiliac joint, depending on which is located more caudally. The anal canal was contoured from the external sphincter up to the internal sphincter (typically 3 cm). The blad-

der was defined by the external wall, delineated on each slide from the dome to the base. The sigmoid was defined by the rectosigmoid flexure to the part where the intestinal structure deflects in cranial direction (in the sagittal view). The femoral heads were caudally delineated until the trochanter minor. The small bowel included the individual bowel loop from the duodenum to the ileocecal junction. The small bowel was only contoured when located near the PTV (till 2 cm above delineated PTV). The penile bulb was delineated as that portion of the bulbus spongiosum of the penis immediately inferior to the urogenital diaphragm. This structure did not extend anteriorly into the shaft or pendulous portion of the penis.

2.2.3 Treatment planning strategy

For every patient a VMAT plan for the Agility (Elekta AB, Stockholm, Sweden) and an IMRT plan for the Unity MR-Linac were created. Total prescribed dose to be delivered in 5 fractions was 36.25 Gy to the PTV_P and 30 Gy to the PTV_{SV}. Planning constraints for coverage of target volumes and OAR are shown in Table 2. Depicted OAR constraints were based on constraints used in the hypo-FLAME study and clinical protocols of the Radiotherapiegroep and Radboudumc [25]. First treatment planning priority was minimizing the dose to the OAR and in particular the rectum and bladder. Second priority was to have at least 98% of the PTV_P and PTV_{SV} to be covered with 95% of the prescribed dose.

2.2.4 Intensity Modulated Radiotherapy

IMRT treatment plans for MR-Linac treatment were created using Monaco v5.40 (Elekta AB, Stockholm, Sweden) treatment planning system (TPS) using an 11 beam setup. Specific MR-Linac beam characteristics and the presence of the magnetic field as well as the cryostat-pipe were accounted for in the TPS. Limitation of small field segments was ensured by a minimum segment area and width of respectively 6 cm² and 0.5 cm. The minimum number of motor units per segment was 4, with a maximum of 50 segments per plan. The treatment plans were generated using a grid size of 0.3 × 0.3 × 0.3 cm, with a statistical uncertainty per calculation of 1%. The MR-Linac has a fixed table top to isocenter distance of 13 cm and a beam photon energy of 10 MV. The first step in the optimization process was to determine a class solution, resulting in a objectives template as a starting point for treatment plan optimization for every individual patient. Clinical target

Table 2: Clinical target and OAR constraints

Structure	Metric	(Iso)dose
PTV _P	V34.44Gy	>98%
	V38.78Gy	<0.1 cc
PTV _{SV}	V28.50Gy	>98%
CTV _P	V34.44Gy	>99%
CTV _{SV}	V28.50Gy	>99%
Rectum	V28Gy	<20%
	V32Gy	<15%
	V35Gy	<2 cc
	V38Gy	<1 cc
Bladder	V28Gy	<20%
	V32Gy	<15%
	V37Gy	<5 cc
Anal canal	Dmean	<20 Gy
Femoral Head	V28Gy	<5 cc
Penile bulb	V20Gy	<90%
Small bowel	V19.50Gy	<5 cc
	V35Gy	<0.1 cc

Dose constraints based on the hypo-FLAME study and clinical protocols of the Radiotherapiegroep and Radboudumc.

and OAR constraints have been taken into account during the design of the solution. To match current clinical standard within Radiotherapiegroep, achievement of dose to target conformity was prioritized in the Monaco optimization process.

2.2.5 Volumetric Arc Therapy

VMAT treatment plans were created using the Monaco v5.40 TPS. Two identical VMAT arcs were planned, accounting for treatment complexity and assessment of intrafraction motion between delivery of both arcs. The starting angle was 160° and the stop angle was 200° (counterclockwise), resulting in a 320° arc. The use of these gantry angles avoids irradiation through the spinal cord. The collimator angle was 5°. The treatment plans were generated using a grid size of 0.3 × 0.3 × 0.3 cm and a gantry spacing of 4°. The photon energy was 10 MV.

2.2.6 Data analysis

MR-Linac IMRT plans were compared to conventional linac VMAT plans using dose-volume histogram (DVH) parameters. The 3D dose distributions were obtained. The aim was to achieve the lowest possible rectal and bladder dose while meeting the dose delivery criteria to the PTV. The DVHs were used for assessing dose to the CTVs and the OAR. To accurately compare the dosimetric impact of MR-Linac IMRT planning to a

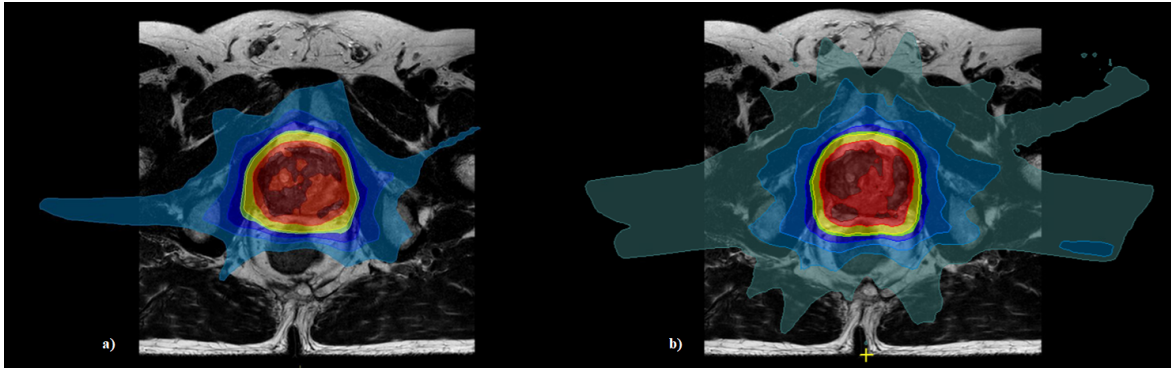


Figure 1: The dose distributions of a) fiducial marker (FM) position verification, b) adaptive replanning using a 5 mm CTV to PTV margin.

conventional linac VMAT across all patients, the dose distribution was normalised so that 95% of the prescribed dose covered 98% of the PTV_P. This guarantees that differences in OAR sparing between modalities are not caused by a difference in target coverage. Paired variables were compared by non-parametric testing using a two-tailed Wilcoxon signed-rank test ($p < 0.1$) within the IBM SPSS Statistics 26 (Chicago, IL, USA) system.

2.3 Results

Table 3 shows the dosimetric results of the conventional linac VMAT treatment plans and the MR-Linac IMRT treatment plans, with corresponding p-values of significance. The prescribed dose of 36.25 Gy to the PTV_P and 30 Gy to the CTV_{SV} was adequately covered for both treatment modalities. The optimization criteria were such that the OAR constraints were met in all patients. PTV_P doses for MR-Linac IMRT remained within the 107% isodose, where conventional linac VMAT showed small volumes of more than 107% of the prescribed dose (0.00 - 0.27 cc) in two patients. However, these violations were considered to be clinically irrelevant since OAR constraints were met for these particular patients. MR-Linac IMRT showed reduced high dose regions, with consequently smaller rectal V35Gy (VMAT: 0.00 - 1.84 cc; IMRT: 0.00 - 1.54 cc). Conventional linac VMAT showed reduced low dose regions, resulting in smaller rectum V28Gy (VMAT: 0.99 - 14.47%; IMRT: 3.02 - 15.44%) and bladder V28Gy (VMAT: 3.81 - 9.52%; IMRT: 3.76 - 13.20%), both statistically significant ($p < 0.1$). The mean dose of the anal canal remained within the 20 Gy isodose for both modalities. However, the mean dose (VMAT: 3.92 - 15.12 Gy; IMRT: 5.10 - 18.26 Gy) increased for the MR-Linac IMRT treatment plans. Additionally, MR-Linac IMRT

showed larger volumes of the penile bulb receiving at least 20 Gy (VMAT: 0.00 - 53.29%; IMRT: 0.00 - 74.62%). That difference remained within the OAR constraint and was not statistically significant ($p > 0.1$). Figure 1 shows a transversal view of a conventional linac VMAT and an MR-Linac IMRT treatment plan for a patient within the study.

2.4 Discussion

The aim of this study was to investigate whether similar dose parameters can be achieved for MR-Linac IMRT planning compared to conventional linac VMAT planning using stereotactic body radiotherapy for PCa treatment. Thereby, taking the treatment planning limitations and presence of the 1.5T magnetic field of the MR-Linac into account. The results show that the OAR constraints for the rectum and bladder were not exceeded for MR-Linac IMRT treatment plans. MR-Linac IMRT showed increased low dose regions, with consequently increased V28Gy of the bladder and rectum. Additionally, the mean dose to the anal canal was increased in all cases during MR-Linac IMRT planning. However, in no case the V28Gy for the rectum and bladder and the Dmean for the anal canal exceeded the clinical constraints. The differences were considered to be clinically acceptable since all OAR constraints were met, despite their statistical significance.

Remarkably, the high dose regions (V35Gy) for the rectum are smaller in the MR-Linac IMRT treatment planning compared to conventional linac VMAT, despite the potential influence of the ERE. The ERE may potentially disturb the dose distribution and cause local hot spots of high radiation dose. This effect is particularly evident at boundaries with major differences in density, such as air-tissue boundaries. Rectal air

Table 3: Dosimetric results of conventional linac VMAT and MR-Linac IMRT treatment plans

	Metric	VMAT		IMRT		p-value
		mean	range	mean	range	
PTV_P	V107% (%)	0.11	(0.00 - 0.27)	0.00	(0.00 - 0.00)	0.500
	Dmean (Gy)	36.48	(35.69 - 36.94)	35.95	(35.80 - 36.19)	0.063
PTV_{vs}	V95% (%)	99.10	(98.25 - 99.76)	99.45	(98.04 - 99.97)	0.625
Rectum	V28Gy (%)	9.40	(0.99 - 14.47)	11.80	(3.02 - 15.44)	0.063
	V32Gy (%)	5.33	(0.11 - 8.98)	6.73	(0.81 - 9.51)	0.063
	V35Gy (cc)	1.12	(0.00 - 1.84)	0.99	(0.00 - 1.54)	0.625
	V38Gy (cc)	0.00	(0.00 - 0.00)	0.00	(0.00 - 0.00)	1.000
Bladder	V28Gy (%)	6.25	(3.81 - 9.52)	7.56	(3.76 - 13.20)	0.125
	V32Gy (%)	4.08	(2.20 - 6.41)	4.73	(1.87 - 8.74)	0.313
	V37Gy (cc)	0.97	(0.00 - 3.97)	0.00	(0.00 - 0.01)	0.125
Anal canal	Dmean (Gy)	9.12	(3.92 - 15.12)	11.33	(5.10 - 18.26)	0.063
Fem. Heads	V28Gy (cc)	0.05	(0.00 - 0.23)	0.00	(0.00 - 0.00)	1.000
Penile Bulb	V20Gy (%)	14.70	(0.00 - 53.29)	27.34	(0.00 - 74.62)	0.125

The dosimetric results for PTV coverage and OAR sparing. The mean values are reported with the corresponding range. The p-value shows the significance level for the difference between conventional linac VMAT and MR-Linac IMRT dose distributions.

cavities are common and can appear during irradiation. High dose regions within the rectal wall are undesirable, since the rectal wall is particularly sensitive to hot spots. To fully account for the ERE, no density override was applied to the rectum. The results indicate no deterioration of the dose distribution at the rectal wall. However, cases included within this study do not show large rectal air pockets at the level of the high dose regions. Previous literature shows that the ERE does affect the dose distribution. Raaijmakers et al. [27] stated that in the presence of a magnetic field with any given magnetic field strength, dose inhomogeneities due to the ERE exist for air cavities with a radius of >1 cm. These findings were confirmed by a planning study in rectal cancer patients by Sripes et al. [28] Locally, the ERE will induce hot spots within 3 mm of the rectal-air interface. However, the use of real-time MR tracking during treatment delivery would allow for early detection of rectal air cavities and treatment termination or adaptation.

The current planning study is a stage 0 radiotherapy predicate study. It addresses how the innovative treatment will be delivered, including development of a planning objective template and the expected quality of dose distributions [21]. Since only five cases were included, no definitive treatment consequences should be drawn from the results. However, it allows prediction of the feasibility of PCa treatment on the MR-Linac and which planning strategies might be suitable for upcoming implementation of the MR-Linac. De-

spite the small number of included subjects, the results of this study are in line with previous literature. Den Hartogh et al. and Tetar et al. both focused on the planning feasibility for the MR-Linac [17][22]. They showed clinically acceptable treatment plans and only small dose differences [17]. However, Den Hartogh et al. and Tetar et al. used two different planning modalities for comparison of conventional linac VMAT and MR-Linac IMRT. Within our study the Monaco V5.40 TPS was used for both conventional linac VMAT and MR-Linac IMRT planning. Therefore, it can be assumed that found differences depend on the limitations of the MR-Linac IMRT modality and the presence of the 1.5T magnetic field and not on the differences in TPS or planning strategy.

The results indicate that MR-Linac IMRT treatment planning yield similar dose distributions as conventional linac VMAT treatment planning. However, not only the dose distribution influences the feasibility of the treatment delivery with the MR-Linac. Treatment times for the MR-Linac IMRT are substantially prolonged as compared to conventional linac VMAT, due to the lower dose rate of the MR-Linac (conventional: 600 MU/min; MR-Linac: 420 MU/min) and IMRT delivery instead of VMAT. With longer treatment times, the probability of intrafraction prostate motion also increases [29]. This effect might necessitate increasing of the CTV to PTV margin. However, available online adaptive replanning and future real-time target tracking might compensate for the adverse effects of prolonged treatment times.

The results of this study allow for further exploration of planning strategies with the MR-Linac, including daily adaptive replanning. An additional stage 0 study implementing daily adaptive replanning has been initiated and might clarify the potential benefit of the MR-Linac for treatment of PCa.

2.5 Conclusion

Stereotactic body radiotherapy treatment planning for PCa on a 1.5T MR-Linac is feasible, resulting in similar dose distributions compared to treatment planning for a conventional linac. Only small differences in target coverage and OAR sparing were found. Further exploration of MR-Linac treatment delivery for PCa, and in particular online adaptive replanning, might clarify the potential benefit for PCa treatment.

3 Towards online adaptive replanning with the Elekta Unity MR-Linac for extremely hypofractionated prostate carcinoma radiotherapy treatment

3.1 Introduction

In recent years, the introduction of improved image guided radiation therapy (IGRT) techniques allowed a new standard fractionation option for PCa in the clinical setting. This is an extremely hypofractionated scheme of 5×7.25 Gray (Gy) for low- and intermediate risk PCa [9][12]. The introduction of such dose escalations has prompted a re-examination of the current radiation techniques to ensure safe escalation of radiation dose [29]. Dose escalations necessitate the reduction of CTV to PTV margins, to minimize the dose to healthy tissue. However, reducing treatment margins may result in unduly compromising radiation of the target volume due to intrafraction motion [29].

Modern EBRT techniques ensure accurate irradiation of the tumor and prostate and sparing of OAR by target position verification based upon the position of gold FMs. By using the FM position on daily CBCT or EPID as a surrogate for the prostate, set-up errors and internal motion of the prostate relative to the bony anatomy can be identified [30]. Since the tumor is surrounded by OAR, particularly the rectal wall and bladder, the targeting of an extremely hypofractionated radiation dose should be accurate. Precision of FM based position verification is high [12]. However, the effectiveness of this method relies on the fixation of the FMs within the prostate, the absence of significant deformation and rotation of the prostate during the course of treatment and the accuracy of marker position verification [30].

Current standard CTV to PTV margin used for treatment of PCa patients in Radiotherapiegroep is a 5 mm isotropic margin. The upcoming introduction of an MR-Linac in the clinical setting offers the possibility to perform daily adaptive replanning and consequently correcting for daily interfraction prostate displacement and deformation. Recent literature suggests even a reduction of that margin to 3 mm, due to daily dose adaptation, improved soft tissue contrast resulting in more accurate patient positioning and potential real-time target tracking [17][29][31].

The concept of daily adaptive replanning with the Unity MR-Linac (Elekta AB, Stockholm, Sweden) is plan adaptation during every treatment frac-

tion, with an ‘adapt-to-position’ (ATP) and an ‘adapt-to-shape’ (ATS) method available. The ATP method only adapts the treatment plan isocenter position, thus requires no daily delineation. The ATS workflow requires daily delineation and adapts the plan to all deformations of the anatomy. Both options recalculate or re-optimize the pre-treatment plan to reproduce or improve target coverage and OAR sparing. The ATS workflow is significantly more time consuming, due to daily recontouring and replanning. However, Winkel et al. found that only full online replanning using the ATS workflow can produce clinically acceptable treatment plans for PCa. Violations for the ATS workflow were often caused by insufficient target coverage or insufficient OAR sparing. [23]

This study is a R-IDEAL stage 0 study unraveling the available full online adaptive planning strategy available in the Unity MR-Linac workflow [21]. A comparison is made between current FM based position verification and daily adaptive replanning for PCa radiotherapy treatment. In this work, treatment planning for the Unity MR-Linac is carried out and potential margin reduction is investigated.

3.2 Methods and materials

3.2.1 Patients

Data of five randomly selected patients treated within the hypo-FLAME study at the University Medical Centre Utrecht was available for this retrospective treatment planning study [25]. The hypo-FLAME study was approved by the institutional review board and informed consent included approval to use the acquired data for future studies. For each included patient, a planning CT and MRI were available. For each of five treatment fractions, a T1-weighted MRI for marker position verification and a T2-weighted MRI for adaptive replanning were acquired. Due to incomplete representation of the target area and surrounding OAR within the planning MRI, the planning MRI was discarded. The MRI of the first fraction was used for pre-treatment planning. The remaining four MRI scans were used for simulation of adaptive replanning.

3.2.2 Radiotherapy simulation and contouring

Prior to radiotherapy treatment, four gold FMs were implanted in the prostate by the radiation oncologist using ultrasound guidance. A planning CT and MRI scan are performed in supine position. Patients were advised to have a comfortably full bladder prior to planning CT and MRI acquisition. The planning CT was rigidly registered with the MRI based on the FMs for delineation of the prostate and OAR.

The different volumes of interest were defined in agreement with ICRU 62 [26]. To minimize possible errors for both the delineation of the prostate and the relevant normal tissues from interobserver variation, all target volumes were delineated by one observer and this delineation was supervised by a radiation oncologist. The prostate gland as visible on MRI was contoured as gross tumor volume prostate (GTV_P) and the clinical target volume prostate (CTV_P) was defined as GTV_P + 0 mm margin. In all five cases seminal vesicle (SV) invasion was present, necessitating delineation of the GTV_{SV}. The GTV_{SV} included the base of the SV plus any region at risk of microscopic extension. The base of the SV was defined as the 2 cm of the SV from the base of the prostate in the axial view. The CTV_{SV} was defined as GTV_{SV} + 0 mm margin. The CTV_P and CTV_{SV} were defined by the observer supervised by the radiation oncologist, based on clinical findings and the planning MRI. To facilitate investigation of margin reduction, PTV_{P+5mm} and PTV_{SV+5mm} include a CTV + 5 mm margin and PTV_{P+3mm} and PTV_{SV+3mm} include a CTV + 3 mm margin.

Delineation of the organs at risk included the rectum, anal canal, bladder, penile bulb, sigmoid, femoral heads and the small bowel. The anorectal contour was defined by the external sphincter to the rectosigmoid flexure or the level of the inferior border of the sacroiliac joint, depending on which is located more caudally. The anal canal was contoured from the external sphincter up to the internal sphincter (typically 3 cm). The bladder was defined by the external wall, delineated on each slide from the dome to the base. The sigmoid was defined by the rectosigmoid flexure to the part where the intestinal structure deflects in cranial direction (in the sagittal view). The femoral heads were caudally delineated until the trochanter minor. The small bowel included the individual bowel loop from the duodenum to the ileocecal junction. The small bowel was only contoured when located near the PTV (till 2 cm

above delineated PTV). The penile bulb was delineated as that portion of the bulbous spongiosum of the penis immediately inferior to the urogenital diaphragm. This structure did not extend anteriorly into the shaft or pendulous portion of the penis.

3.2.3 Pre-treatment planning strategy

For every subject a pre-treatment IMRT plan for the Unity MR-Linac was created. Total prescribed dose to be delivered in 5 fractions was 36.25 Gy to the PTV_P and 30 Gy to the PTV_{SV}. Planning constraints for coverage of target volumes and OAR are shown in Table 4. Depicted OAR constraints were based on constraints used in the hypo-FLAME study and clinical protocols of the Radboudumc and Radiotherapiegroep [25]. First treatment planning priority was minimizing the dose to the OAR and in particular the rectum and bladder. Second priority was to have at least 98% of the PTV_P and PTV_{SV} to be covered with 95% of the prescribed dose.

Table 4: Clinical target and OAR constraints

Structure	Metric	(Iso)dose
PTV _P	V34.44Gy	>98%
	V38.78Gy	<0.1 cc
PTV _{VS}	V28.50Gy	>98%
CTV _P	V34.44Gy	>99%
CTV _{VS}	V28.50Gy	>99%
Rectum	V28Gy	<20%
	V32Gy	<15%
	V35Gy	<2 cc
	V38Gy	<1 cc
Bladder	V28Gy	<20%
	V32Gy	<15%
	V37Gy	<5 cc
Anal canal	Dmean	<20 Gy
Femoral Head	V28Gy	<5 cc
Penile bulb	V20Gy	<90%
Small bowel	V19.50Gy	<5 cc
	V35Gy	<0.1 cc

Dose constraints based on the hypo-FLAME study and clinical protocols of the Radiotherapiegroep and Radboudumc.

IMRT treatment plans for MR-Linac treatment were created using Monaco v5.40 TPS using an 11 beam setup. Specific MR-Linac beam characteristics and the presence of the magnetic field as well as the cryostat-pipe were accounted for in the TPS. Limitation of small field segments was ensured by a minimum segment area and width of respectively 6 cm² and 0.5 cm. The minimum

number of motor units per segment was 4, with a maximum of 50 segments per plan. The treatment plans were generated using a grid size of $0.3 \times 0.3 \times 0.3$ cm, with a statistical uncertainty per calculation of 1%. The MR-Linac has a fixed table top to isocenter distance of 13 cm and a beam photon energy of 10 MV. The class solution for the optimization objectives was used as a starting point for treatment plan optimization for every individual subject, as shown in Appendix A. Clinical target and OAR constraints have been taken into account during the design of the solution. To match current clinical standard within Radiotherapiegroep, achievement of dose to target conformity was prioritized in the Monaco optimization process.

3.2.4 Fiducial marker based position verification

Current clinical practice is simulated by rigidly registering the dose distribution of the pre-treatment plan to the daily MRI. The rigid registration is based upon FM position verification, including translation and omitting rotation.

3.2.5 Adaptive treatment planning strategy

Daily online plan adaptation is simulated by full online replanning including 'optimizing weights and shapes from fluence'. A radiotherapy fraction for the Unity MR-Linac starts with the acquisition of an online MRI. The pre-treatment MRI, contours and plan, together with the online MRI are used as input to adapt the treatment plan to the daily anatomy. The daily MRI is aligned with the pre-treatment MRI using rigid registration based on a volume of interest surrounding the target. After registration, the ATS workflow requires online recontouring of the daily anatomy to fully account for deformations of the prostate and OAR. Electron densities (ED) are determined by the average ED value of each structure on the pre-treatment CT. Assignment of correct ED values is crucial, since optimization of the treatment plan is done using the daily MRI. The pre-treatment planning objectives are a starting point for optimization in the ATS workflow. [23]

3.2.6 Dosimetric evaluation

Dose distributions obtained during simulation of online adaptive replanning were compared to dose distributions obtained during simulation of FM based position verification using dose-volume histogram (DVH) parameters. The 3D dose distributions were obtained. The aim was to achieve

the lowest possible rectal and bladder dose while meeting the dose delivery criteria to the PTV_P and PTV_{SV}. The DVHs were used for assessing dose to the CTVs and the OAR. The primary endpoints assessed were the D2cc to the rectum and bladder. The hypothesis is that the rectal and bladder D2cc of daily adaptive MR-Linac based RT compared to the conventional linac CBCT based RT with position verification based upon FM position will be reduced due to the ability to reduce treatment margins caused by the improved precision in patient positioning. Secondary endpoints included the D50% of the rectum and bladder, the Dmean of the anal canal and (if delineated) the D2cc of the small bowel.

Paired variables were compared by non-parametric testing using a two-tailed Wilcoxon signed-rank test ($p < 0.1$) within the IBM SPSS Statistics 26 (Chicago, IL, USA) system.

3.3 Results

The prescribed dose of 36.25 Gy to the PTV_{P+5mm} and PTV_{P+3mm} and 30 Gy to the PTV_{SV+5mm} and PTV_{SV+3mm} was adequately covered for every case in adaptive replanning. FM position verification showed lack of PTV_{P+5mm} coverage in all subjects. The coverage of the PTV_{P+5mm} and PTV_{P+3mm} was normalised such that 98% of the volume received 95% of the prescribed dose. After normalisation, PTV_{P+5mm} and PTV_{SV+5mm} were both adequately covered for FM based position verification. Table 5 shows the dosimetric results of FM based position verification and adaptive replanning for the MR-Linac using respectively a 5 mm and a 3 mm CTV to PTV margin.

Adaptive replanning using a 5 mm CTV to PTV margin showed reduced high dose regions compared to FM planning, resulting in significant lower rectal D2cc (FM: 28.59 - 37.36 Gy; AR: 27.98 - 34.36 Gy). FM based position verification yielded a maximum mean bladder D2cc of 38.07 Gy, where maximum mean bladder D2cc for adaptive replanning was 36.06 Gy. The difference in mean bladder D2cc between both modalities for all patients was not significant ($p > 0.1$). The minimum dose to 50% of the rectal volume (D50%) was significantly lower for adaptive replanning using a 5 mm CTV to PTV margin (FM: 10.15 - 18.51 Gy; AR: 9.97 - 13.72 Gy), where D50% of the bladder showed no difference between modalities (FM: 2.07 - 5.15 Gy; AR: 2.10 - 6.36 Gy). The mean anal canal dose was reduced for adaptive replanning using a 5mm CTV to PTV margin in four subjects (FM: 6.68 - 16.56 Gy; AR: 7.25 -

Table 5: Dosimetric results of fiducial marker (FM) position verification and adaptive replanning (AR)

Patient	Plan	Rectum		Bladder		Anal canal
		D2cc (Gy)	D50% (Gy)	D2cc (Gy)	D50% (Gy)	Dmean (Gy)
1	FM	37.36	18.51	38.07	5.15	12.61
	AR + 5mm	34.35	13.72	36.06	6.36	8.36
	AR + 3mm	32.96	10.79	35.23	4.48	6.09
2	FM	28.59	11.52	34.70	3.31	15.30
	AR + 5mm	27.98	10.04	34.99	3.24	13.73
	AR + 3mm	24.53	9.39	33.49	2.63	11.69
3	FM	33.44	12.32	36.78	2.07	6.68
	AR + 5mm	32.81	11.79	34.53	2.10	7.25
	AR + 3mm	30.33	9.64	32.46	1.58	5.18
4	FM	35.69	14.24	32.31	3.09	13.30
	AR + 5mm	34.61	13.15	35.46	3.83	12.79
	AR + 3mm	33.08	11.14	34.83	2.31	9.83
5	FM	34.90	10.15	36.05	3.27	16.56
	AR + 5mm	34.36	9.97	35.55	2.69	16.14
	AR + 3mm	33.00	9.93	34.22	2.27	13.16
p-value	FM vs 5mm	0.063	0.063	0.813	0.625	0.313
	5mm vs 3mm	0.063	0.063	0.063	0.063	0.063

FM = fiducial marker; AR+5mm = adaptive replanning using a 5 mm CTV to PTV margin; AR+3mm = adaptive replanning using a 3 mm CTV to PTV margin. The mean dose of FM based position verification and adaptive replanning for rectum D2cc and D50%, bladder D2cc and D50% and anal canal Dmean.

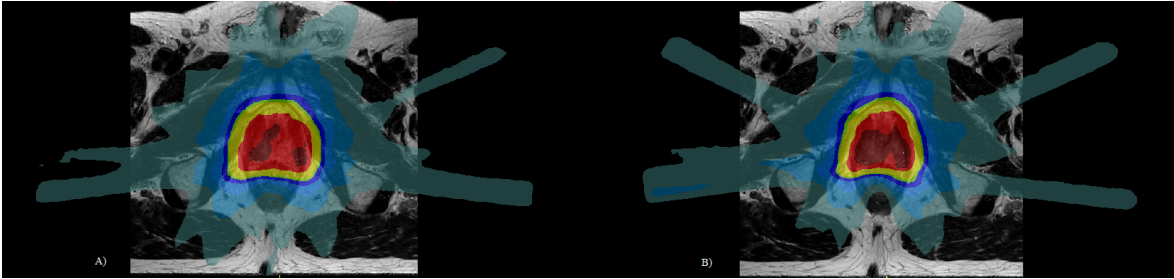


Figure 2: The dose distributions of a) fiducial marker (FM) position verification and b) adaptive replanning (AR) using a 5 mm CTV to PTV margin.

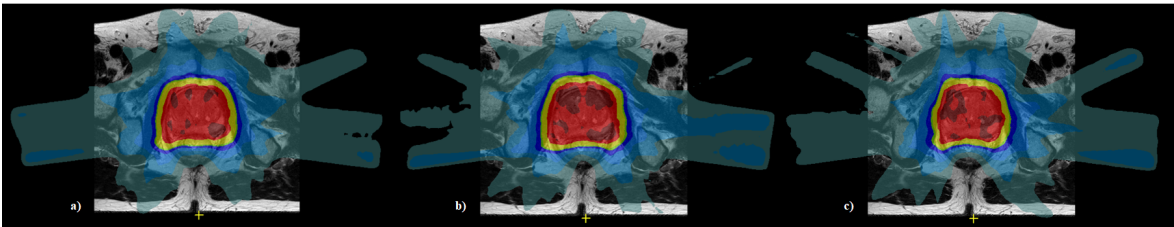


Figure 3: The dose distributions of a) fiducial marker (FM) position verification, b) adaptive replanning (AR) using a 5 mm CTV to PTV margin and c) AR using a 3 mm CTV to PTV margin.

16.14 Gy), although not statistically significant. Figure 2 shows a transverse view of dose distributions obtained with FM based position verification and adaptive replanning based upon a 5 mm CTV to PTV margin.

The dosimetric results of adaptive replanning for the MR-Linac using a 3 mm CTV to PTV margin are also depicted in Table 5. Adapted treatment plans using a 3 mm CTV to PTV margin showed reduced dose to the OAR when compared to adapted treatment plans using a 5 mm CTV to PTV margin. The rectal D2cc and D50%, the bladder D2cc and D50% and the Dmean of the anal canal were significantly lower in the 3 mm treatment plans. Figure 3 shows a transverse view of of dose distributions obtained with FM based position verification and adaptive replanning using respectively a 5 mm PTV margin and a 3 mm CTV to PTV margin.

3.4 Discussion

The aim of this study was to investigate the feasibility of online adaptive replanning and consequently the impact on the dose distribution. Thereby, taking the potential CTV to PTV margin reduction account. The results of this study show that the OAR constraints for the rectum were reduced for Unity MR-Linac adaptive treatment plans. Therefore, MR-Linac potentially reduces rectum toxicity in treatment of PCa.

To estimate and compare the dosimetric impact of daily online adaptive RT, the D2cc was used as primary endpoint. The D2cc is one of the most commonly used parameters for evaluation of rectal and bladder doses. Several studies on toxicity and quality of life after stereotactic ablative radiotherapy of the prostate used D2cc of the rectum and bladder as a dosimetric predictor, e.g. [32]. Alayed et al. have investigated the predictive value of the rectum and bladder D2cc (among others) for late toxicity by analysis of a pooled cohort of patients from four phase II trials. The bladder D2cc remained a significant predictor for grade ≥ 1 and grade ≥ 2 late bladder toxicity. For rectum toxicity, D2cc was found to be a significant predictor as well for late grade ≥ 1 and grade ≥ 2 toxicity. [33] They recommended to apply a bladder dose dose-constraint of D2cc < 39 Gy and a rectal dose-constraint of D2cc < 38 Gy to mitigate late grade ≥ 2 toxicity.

In this study, none of the cases in both modalities exceeded those dose-constraints for rectum and bladder. However, adaptive replanning did show

significant lower D2cc for the rectum. That reduction in D2cc is deemed clinically relevant, since De Boer et al. found higher odds of grade ≥ 2 rectal toxicity per increase in rectal dose of 1 Gy. They also found an association with proctitis and fecal incontinence for rectal D50%. In the current study, the D50% of the rectum is significantly lowered for adaptive replanning when compared to FM based position verification, indicating a potential benefit for toxicity outcomes.

Furthermore, the results of this study indicate that the use of a 3 mm CTV to PTV margin is beneficial for OAR sparing compared to the use of a 5 mm CTV to PTV margin. Due to improved soft tissue contrast of the Unity MR-Linac, target coverage could be ensured. Tetar et al. reported the use of 3 mm CTV to PTV margin for treatment of PCa using online adaptive MR-guidance with gating. However, real-time gating is not yet available on the Unity MR-Linac modality. This might be limiting to CTV to PTV margin reduction, due to the inability to automatically track real-time prostate position. The replanning process is considerably more time consuming than standard conventional position verification based upon FMs. The process including MR acquisition, recontouring, replanning and treatment delivery can take up to 45 minutes. This results in increased probability of intrafraction patient movement or prostate displacement due to differences in rectal or bladder filling. Considering the effect of prostate displacement, there might be a risk of adverse dosimetric effects including less effective targeting. Hypofractionation schedules using small CTV to PTV margins increase that risk even further.

The current planning study is a stage 0 radiotherapy predicate study. The study focuses on the potential benefit in OAR sparing for the treatment of PCa using a extremely hypofractionated dose delivery, including assessment of potential margin reduction. The study gives an indication of the expected dose distributions and potential technical challenges. [21] Due to the small number of patients included, no definitive treatment consequences should be drawn from the study. However, the study allows prediction of the feasibility of PCa treatment on the MR-Linac and which planning strategies might be suitable for upcoming implementation of the MR-Linac. Despite the small number of included subjects, the results of this study are in line with previous literature focused on the online adaptive replanning feasibility for the MR-Linac, such as Deutschmann et al. [31]

They showed clinically acceptable treatment plans and improved healthy tissue sparing using adaptive replanning on the Unity MR-Linac. To the best of our knowledge, this study is the first study quantifying the potential dosimetric consequences of SABR adaptive replanning for PCa treatment with the Unity MR-Linac.

3.5 Conclusion

Adaptive replanning for PCa treatment using the Unity MR-Linac shows reduced high dose regions, with consequently a reduction in rectum and bladder D2cc. Further beneficial innovation includes diminishing of the CTV to PTV margin. However, real-time target and OAR position gating should be available before implementation in the clinical setting.

4 Conclusion

The aim of this thesis was to facilitate a science-based introduction of the MR-Linac for PCa within the clinical setting. The results of this study show that extremely hypofractionated IMRT treatment planning in PCa on an MR-Linac is feasible and potentially yields similar dose distributions as conventional linac VMAT treatment planning. This indicates that the technical differences of the MR-Linac do not lead to a clinically relevant deterioration of the dose distribution. However, prolonged treatment times for the MR-Linac may result in an increase of intrafraction prostate motion [29]. This effect might necessitate increasing of the CTV to PTV margin. However, available online adaptive replanning and future real-time target gating might compensate for the adverse effects of prolonged treatment times.

Within this thesis, adaptive treatment planning led to clinically accepted treatment plans. When comparing adaptive RT with position verification based upon FMs, primary and secondary dose parameters for the rectum were reduced. This indicates a potential dosimetric benefit for adaptive radiotherapy. However, before that conclusion can be drawn, more subject data should be available for analysis.

Furthermore, it is quantified that a diminution of CTV to PTV margins from 5 mm to 3 mm reduces dose to the OAR. The advantage of a 3 mm CTV to PTV margin over a 5 mm CTV to PTV margin is shown by reduced bladder and rectum D2cc and D50%. However, previous literature is clear that intrafraction movement does not allow for a 3 mm CTV to PTV margin unless real-time target gating is available [29].

5 Future perspectives

The conclusion of this thesis stated that adaptive replanning for the MR-Linac shows beneficial OAR sparing compared to conventional FM based position verification. Propagation from a 5 mm to 3 mm CTV to PTV margin can even further increase OAR sparing. Such diminution of CTV to PTV margin can only be realised if target coverage is guaranteed. Developing techniques to make this possible is the main challenge at the moment.

Mannerberg et al. showed considerable prostate movement during a time frame relevant to delivery of single fraction on the Unity MR-Linac [29]. The probability of prostate motion increases over time [34][35]. It is important to obtain information about the target position during irradiation to avoid excessive irradiation of the OAR. Additionally, real-time tracking of the target position is crucial to ensure adequate target coverage, especially when a 3 mm CTV to PTV margin is used.

The use of cine MRI during beam-on enables the option to intervene when disproportional prostate movement is observed [36]. However, this process depends on intervention of an observer. De Muinck Keizer et al. have developed an automatic method to determine intrafraction motion of the prostate based upon FM position on cine MRI [37]. This method allows real-time target gating based on a gating boundary of 3 mm during beam-on time. They found the need for 2D shifts updating target position in >20% of all delivered fractions, implicating the need for target gating options. However, real-time target gating is not yet available for the Unity MR-Linac.

A second approach to diminishing CTV to PTV margins is to minimize the positioning error prior to irradiation. Currently, a planning CT is needed for ED calculations and is rigidly registered to the planning MRI. The advantages of an MR-only workflow includes reduction of dosimetric errors caused by inaccurate rigid registration with the planning CT or temporal changes in anatomy between the planning CT and MRI. An MR-only workflow requires the acquisition of synthetic CT images. Recently, the first commercial synthetic CT software MR for Calculation Attenuation (MRCAT) became available [38] and is compatible with the Unity MR-Linac. Tyagi et al. performed validation of MRCAT including dosimetric validation between CT and MRCAT and found no significant difference between dose distribution based upon MRCAT compared to CT. Future research must quantify the accuracy in treatment positioning based upon MR-only.

The use of both real-time gating and the MRI-only workflow might potentially enable the use of a 3 mm CTV to PTV margin, resulting in improved OAR sparing. Additionally, further dose escalation becomes a possibility. With a low estimated α/β ratio, even further hypofractionation schedules would be beneficial. The use of SBRT (≥ 7.0 Gy per fraction) shows improved clinical outcomes and improved patient contentment [39]. The hypo-FLAME study has reported favorable biochemical outcomes for low, intermediate and high risk patients. Further dose escalation could be provided by personalized treatment, including delivery of an ablative boost to the most aggressive part of the lesion. That intraprostatic lesion is the most common site of local recurrence. Diffusion weighted imaging is able to identify that specific region within the prostate. [25]

The hypo-FLAME study has proven that delivery of such extremely hypofractionated schedules is safe and effective. Even further dose escalation might be beneficial, e.g. in case of radiorecurrent localized PCa. High fraction dose is already clinically available when patients are treated with high-dose-rate brachytherapy (HDR-BT). Hoskin et al. reported fraction schedules for HDR-BT of a single fraction at 19 Gy, showing acceptable toxicity rates [40]. Prada et al. showed a favorable biochemical control rate of 66% at 6 years after treatment [41]. Although brachytherapy (BT) is seen as favorable in conformal treatment, the procedure is invasive and not all patients are eligible for BT. Willigenburg et al. compared HDR-BT and MR-Linac dose distributions for a single fraction of 19 Gy. They found that similar a single fraction 19 Gy treatment is feasible for the MR-Linac and obtained similar dose distributions for the MR-Linac compare to HDR-BT. The major limitation for introduction of the technique is also in this case the lack of real-time gating. [42]

In conclusion, the MR-Linac has great potential for treatment of PCa, including diminution of radiotherapy margins and further dose escalation. To ensure safe introduction of those techniques, it is crucial that real-time target gating becomes available.

References

- [1] N. Mottet, R. van den Bergh, and E. Briers, “EAU Guidelines edn. presented at the EAU Annual Congress Barcelona,” 2019.
- [2] E. Hamoen and F. Witjes, “Behandeling gelokaliseerd prostaatkarcinoom,” *Huisarts en wetenschap*, vol. 55, no. 5, pp. 222–224, 2012.
- [3] R. G. Cremers, M. H. Blanker, and M. M. Bloemendal, “Wat als prostaatkanker in de familie voorkomt?,” *Tijdschrift voor Urologie*, vol. 10, no. 2, pp. 22–29, 2020.
- [4] T. M. de Reijke, J. Battermann, R. van Moorselaar, I. Jong, A. Visser, and J. Burgers, “Richtlijn ‘Prostaatkarcinoom: diagnostiek en behandeling’,” *Nederlands Tijdschrift voor Geneeskunde*, vol. 152, no. 32, pp. 1771–1775, 2008.
- [5] S. M. Camps, D. Fontanarosa, F. Verhaegen, B. G. Vanneste, *et al.*, “The use of ultrasound imaging in the external beam radiotherapy workflow of prostate cancer patients,” *BioMed research international*, vol. 2018, 2018.
- [6] C. Rasch, I. Barillot, P. Remeijer, A. Touw, M. van Herk, and J. V. Lebesque, “Definition of the prostate in CT and MRI: a multi-observer study,” *International Journal of Radiation Oncology* Biology* Physics*, vol. 43, no. 1, pp. 57–66, 1999.
- [7] U. A. van der Heide, A. N. Kotte, H. Dehdad, P. Hofman, J. J. Lagenijk, and M. van Vulpen, “Analysis of fiducial marker-based position verification in the external beam radiotherapy of patients with prostate cancer,” *Radiotherapy and oncology*, vol. 82, no. 1, pp. 38–45, 2007.
- [8] A. U. Kishan, A. Dang, A. J. Katz, C. A. Mantz, S. P. Collins, N. Aghdam, F.-I. Chu, I. D. Kaplan, L. Appelbaum, D. B. Fuller, *et al.*, “Long-term outcomes of stereotactic body radiotherapy for low-risk and intermediate-risk prostate cancer,” *JAMA network open*, vol. 2, no. 2, pp. e188006–e188006, 2019.
- [9] G. Kothari, A. Loblaw, A. C. Tree, N. J. van As, D. Moghanaki, S. S. Lo, P. Ost, and S. Siva, “Stereotactic body radiotherapy for primary prostate cancer,” *Technology in cancer research & treatment*, vol. 17, p. 1533033818789633, 2018.
- [10] A. Katz, “Stereotactic body radiotherapy for low-risk prostate cancer: a ten-year analysis,” *Cureus*, vol. 9, no. 9, 2017.
- [11] A. Widmark, A. Gunnlaugsson, L. Beckman, C. Thellenberg-Karlsson, M. Hoyer, M. Lagerlund, P. Fransson, J. Kindblom, C. Ginman, B. Johansson, *et al.*, “Extreme hypofractionation versus conventionally fractionated radiotherapy for intermediate risk prostate cancer: early toxicity results from the Scandinavian randomized phase iii trial “HYPO-RT-PC”,” *International Journal of Radiation Oncology, Biology, Physics*, vol. 96, no. 5, pp. 938–939, 2016.
- [12] A. Widmark, A. Gunnlaugsson, L. Beckman, C. Thellenberg-Karlsson, M. Hoyer, M. Lagerlund, J. Kindblom, C. Ginman, B. Johansson, K. Björnlinger, *et al.*, “Ultra-hypofractionated versus conventionally fractionated radiotherapy for prostate cancer: 5-year outcomes of the HYPO-RT-PC randomised, non-inferiority, phase 3 trial,” *The Lancet*, vol. 394, no. 10196, pp. 385–395, 2019.
- [13] T. F. Mutanga, H. C. de Boer, G. J. van der Wielen, D. Wentzler, J. Barnhoorn, L. Incrocci, and B. J. Heijmen, “Stereographic targeting in prostate radiotherapy: speed and precision by daily automatic positioning corrections using kilovoltage/megavoltage image pairs,” *International Journal of Radiation Oncology, Biology, Physics*, vol. 71, no. 4, pp. 1074–1083, 2008.
- [14] A. J. McPartlin, X. Li, L. E. Kershaw, U. Heide, L. Kerkmeijer, C. Lawton, U. Mahmood, F. Pos, N. van As, M. van Herk, *et al.*, “MRI-guided prostate adaptive radiotherapy—a systematic review,” *Radiotherapy and Oncology*, vol. 119, no. 3, pp. 371–380, 2016.

- [15] R. L. Christiansen, C. R. Hansen, R. H. Dahlrot, A. S. Bertelsen, O. Hansen, C. Brink, and U. Bernchou, “Plan quality for high-risk prostate cancer treated with high field magnetic resonance imaging guided radiotherapy,” *Physics and imaging in radiation oncology*, vol. 7, pp. 1–8, 2018.
- [16] B. Raaymakers, J. Lagendijk, J. Overweg, J. Kok, A. Raaijmakers, E. Kerkhof, R. Van Der Put, I. Meijsing, S. Crijns, F. Benedosso, *et al.*, “Integrating a 1.5 T MRI scanner with a 6 MV accelerator: proof of concept,” *Physics in Medicine & Biology*, vol. 54, no. 12, p. N229, 2009.
- [17] S. U. Tetar, A. M. Bruynzeel, F. J. Lagerwaard, B. J. Slotman, O. Bohoudi, and M. A. Palacios, “Clinical implementation of magnetic resonance imaging guided adaptive radiotherapy for localized prostate cancer,” *Physics and Imaging in Radiation Oncology*, vol. 9, pp. 69–76, 2019.
- [18] S. Crijns, B. Raaymakers, and J. Lagendijk, “Proof of concept of MRI-guided tracked radiation delivery: tracking one-dimensional motion,” *Physics in Medicine & Biology*, vol. 57, no. 23, p. 7863, 2012.
- [19] C. Peng, E. Ahunbay, G. Chen, S. Anderson, C. Lawton, and X. A. Li, “Characterizing inter-fraction variations and their dosimetric effects in prostate cancer radiotherapy,” *International Journal of Radiation Oncology, Biology, Physics*, vol. 79, no. 3, pp. 909–914, 2011.
- [20] J. J. Lagendijk, B. W. Raaymakers, A. J. Raaijmakers, J. Overweg, K. J. Brown, E. M. Kerkhof, R. W. van der Put, B. Hårdemark, M. van Vulpen, and U. A. van der Heide, “MRI/linac integration,” *Radiotherapy and Oncology*, vol. 86, no. 1, pp. 25–29, 2008.
- [21] H. M. Verkooijen, L. G. Kerkmeijer, C. D. Fuller, R. Huddart, C. Faivre-Finn, M. Verheij, S. Mook, A. Sahgal, E. Hall, and C. Schultz, “R-IDEAL: a framework for systematic clinical evaluation of technical innovations in radiation oncology,” *Frontiers in oncology*, vol. 7, p. 59, 2017.
- [22] D. de Muinck Keizer, L. Kerkmeijer, T. Willigenburg, A. van Lier, M. den Hartogh, J. v. d. V. van Zyp, E. de Groot-van Breugel, B. Raaymakers, J. Lagendijk, and J. de Boer, “Prostate intrafraction motion during the preparation and delivery of MR-guided radiotherapy sessions on a 1.5 T MR-Linac,” *Radiotherapy and Oncology*, vol. 151, pp. 88–94, 2020.
- [23] D. Winkel, G. H. Bol, P. S. Kroon, B. van Asselen, S. S. Hackett, A. M. Werensteijn-Honingh, M. P. Intven, W. S. Eppinga, R. H. Tijssen, L. G. Kerkmeijer, *et al.*, “Adaptive radiotherapy: the Elekta Unity MR-linac concept,” *Clinical and translational radiation oncology*, vol. 18, pp. 54–59, 2019.
- [24] A. Raaijmakers, B. W. Raaymakers, S. van der Meer, and J. J. Lagendijk, “Integrating a MRI scanner with a 6 MV radiotherapy accelerator: impact of the surface orientation on the entrance and exit dose due to the transverse magnetic field,” *Physics in Medicine & Biology*, vol. 52, no. 4, p. 929, 2007.
- [25] C. Draulans, U. A. van der Heide, K. Haustermans, F. J. Pos, J. v. d. V. van Zyp, H. De Boer, V. H. Groen, E. M. Monnikhof, R. J. Smeenk, M. Kunze-Busch, *et al.*, “Primary endpoint analysis of the multicentre phase II hypo-FLAME trial for intermediate and high risk prostate cancer,” *Radiotherapy and Oncology*, vol. 147, pp. 92–98, 2020.
- [26] S. Morgan-Fletcher, “Prescribing, recording and reporting photon beam therapy (Supplement to ICRU Report 50), ICRU Report 62. ICRU, pp. ix+ 52, 1999 (ICRU Bethesda, MD) 65.00 ISBN 0-913394-61-0,” 2001.
- [27] A. Raaijmakers, B. W. Raaymakers, and J. J. Lagendijk, “Magnetic-field-induced dose effects in MR-guided radiotherapy systems: dependence on the magnetic field strength,” *Physics in Medicine & Biology*, vol. 53, no. 4, p. 909, 2008.
- [28] P. G. Sripes, E. Subashi, S. Burlison, J. Liang, P. Romesser, C. Crane, J. Mechalakos, M. Hunt, and N. Tyagi, “Impact of varying air cavity on planning dosimetry for rectum patients treated on a 1.5 T hybrid MR-linac system,” *Journal of Applied Clinical Medical Physics*, 2020.

- [29] A. Mannerberg, E. Persson, J. Jonsson, C. J. Gustafsson, A. Gunnlaugsson, L. E. Olsson, and S. Ceberg, “Dosimetric effects of adaptive prostate cancer radiotherapy in an MR-linac workflow,” *Radiation Oncology*, vol. 15, no. 1, pp. 1–9, 2020.
- [30] E. M. Quan, X. Li, Y. Li, X. Wang, R. J. Kudchadker, J. L. Johnson, D. A. Kuban, A. K. Lee, and X. Zhang, “A comprehensive comparison of IMRT and VMAT plan quality for prostate cancer treatment,” *International Journal of Radiation Oncology, Biology, Physics*, vol. 83, no. 4, pp. 1169–1178, 2012.
- [31] H. Deutschmann, G. Kametriser, P. Steininger, P. Scherer, H. Schöller, C. Gaisberger, M. Mooslechner, B. Mitterlechner, H. Weichenberger, G. Fastner, *et al.*, “First clinical release of an online, adaptive, aperture-based image-guided radiotherapy strategy in intensity-modulated radiotherapy to correct for inter-and intrafractional rotations of the prostate,” *International Journal of Radiation Oncology, Biology, Physics*, vol. 83, no. 5, pp. 1624–1632, 2012.
- [32] Y. Alayed, P. Cheung, D. Vesprini, S. Liu, W. Chu, H. Chung, H. B. Musunuru, M. Davidson, A. Ravi, L. Ho, *et al.*, “SABR in high-risk prostate cancer: outcomes from 2 prospective clinical trials with and without elective nodal irradiation,” *International Journal of Radiation Oncology, Biology, Physics*, vol. 104, no. 1, pp. 36–41, 2019.
- [33] Y. Alayed, M. Davidson, H. Quon, P. Cheung, W. Chu, H. T. Chung, D. Vesprini, A. Ong, A. Chowdhury, S. K. Liu, *et al.*, “Dosimetric predictors of toxicity and quality of life following prostate stereotactic ablative radiotherapy,” *Radiotherapy and Oncology*, vol. 144, pp. 135–140, 2020.
- [34] M. J. Ghilezan, D. A. Jaffray, J. H. Siewerdsen, M. Van Herk, A. Shetty, M. B. Sharpe, S. Z. Jafri, F. A. Vicini, R. C. Matter, D. S. Brabbins, *et al.*, “Prostate gland motion assessed with cine-magnetic resonance imaging (cine-MRI),” *International Journal of Radiation Oncology, Biology, Physics*, vol. 62, no. 2, pp. 406–417, 2005.
- [35] K. M. Langen, T. R. Willoughby, S. L. Meeks, A. Santhanam, A. Cunningham, L. Levine, and P. A. Kupelian, “Observations on real-time prostate gland motion using electromagnetic tracking,” *International Journal of Radiation Oncology, Biology, Physics*, vol. 71, no. 4, pp. 1084–1090, 2008.
- [36] J. Murray and A. C. Tree, “Prostate cancer—advantages and disadvantages of MR-guided RT,” *Clinical and translational radiation oncology*, vol. 18, pp. 68–73, 2019.
- [37] D. de Muinck Keizer, A. Pathmanathan, A. Andreychenko, L. Kerkmeijer, J. v. d. V. van Zyp, A. Tree, C. van den Berg, and J. de Boer, “Fiducial marker based intra-fraction motion assessment on cine-MR for MR-linac treatment of prostate cancer,” *Physics in Medicine & Biology*, vol. 64, no. 7, p. 07NT02, 2019.
- [38] N. Tyagi, S. Fontenla, M. Zelefsky, M. Chong-Ton, K. Ostergren, N. Shah, L. Warner, M. Kadbi, J. Mechalakos, and M. Hunt, “Clinical workflow for MR-only simulation and planning in prostate,” *Radiation Oncology*, vol. 12, no. 1, p. 119, 2017.
- [39] A. U. Pathmanathan, N. J. van As, L. G. Kerkmeijer, J. Christodouleas, C. A. Lawton, D. Vesprini, U. A. van der Heide, S. J. Frank, S. Nill, U. Oelfke, *et al.*, “Magnetic resonance imaging-guided adaptive radiation therapy: a “game changer” for prostate treatment?,” *International Journal of Radiation Oncology, Biology, Physics*, vol. 100, no. 2, pp. 361–373, 2018.
- [40] P. Hoskin, A. Rojas, P. Ostler, R. Hughes, R. Alonzi, and G. Lowe, “Single-dose high-dose-rate brachytherapy compared to two and three fractions for locally advanced prostate cancer,” *Radiotherapy and Oncology*, vol. 124, no. 1, pp. 56–60, 2017.
- [41] P. J. Prada, I. Jimenez, H. González-Suárez, J. Fernández, C. Cuervo-Arango, and L. Mendez, “High-dose-rate interstitial brachytherapy as monotherapy in one fraction and transperineal hyaluronic acid injection into the perirectal fat for the treatment of favorable stage prostate cancer: treatment description and preliminary results,” *Brachytherapy*, vol. 11, no. 2, pp. 105–110, 2012.

- [42] T. Willigenburg, E. Beld, J. Hes, J. J. Lagendijk, H. C. de Boer, M. A. Moerland, *et al.*, “Focal salvage treatment for radiorecurrent prostate cancer: A magnetic resonance-guided stereotactic body radiotherapy versus high-dose-rate brachytherapy planning study,” *Physics and Imaging in Radiation Oncology*, vol. 15, pp. 60–65, 2020.